Chemistry & Biology
Review

Energy Conversion in Natural and Artificial Photosynthesis

Iain McConnell, Gonghu Li, and Gary W. Brudvig*
Department of Chemistry, Yale University, New Haven, CT 06520, USA
*Correspondence: gary.brudvig@yale.edu
DOI 10.1016/j.chembiol.2010.05.005

Modern civilization is dependent upon fossil fuels, a nonrenewable energy source originally provided by the storage of solar energy. Fossil-fuel dependence has severe consequences, including energy security issues and greenhouse gas emissions. The consequences of fossil-fuel dependence could be avoided by fuel-producing artificial systems that mimic natural photosynthesis, directly converting solar energy to fuel. This review describes the three key components of solar energy conversion in photosynthesis: light harvesting, charge separation, and catalysis. These processes are compared in natural and in artificial systems. Such a comparison can assist in understanding the general principles of photosynthesis and in developing working devices, including photoelectrochemical cells, for solar energy conversion.

Introduction

As of today, solar energy remains the most abundant renewable energy resource available to us. Yet there is a huge gap between our present use of solar energy and its enormous potential (Lewis, 2007a, 2007b). This potential is demonstrated by the sheer energy throughput of natural photosynthesis, indicating the feasibility of efficient solar energy conversion via photoinduced charge separation. A steadily improving understanding of natural photosynthesis at the molecular level has been assisted and inspired further by the creation of artificial photosynthetic model systems, such as donor–acceptor assemblies. Indeed, a significant amount of research effort has been directed toward the development of artificial systems composed of molecular and supramolecular architectures, as discussed in several relevant reviews (Alstrum-Acevedo et al., 2005; Balzani et al., 2008; Barber, 2009; Hambourger et al., 2009; Herrero et al., 2008).

In nature, light absorption by antenna complexes is followed by efficient charge separation across a membrane via photosynthetic reaction center proteins (RCs). Dye–sensitized solar cells (DSSCs) utilize an analogous mechanism to harvest sunlight and convert solar energy to electricity. In order to use solar energy for fuel production, the light–induced charge separation must be coupled to fuel–forming redox reactions. Study of the oxygen-evolving complex (OEC) in photosystem II (PSII), specifically the Mn_4Ca bioinorganic core, has inspired the design and synthesis of a variety of water–oxidation catalysts based on transition–metal complexes. This in turn has led to efforts to develop photoelectrochemical synthesis cells for solar fuel formation that are constructed by combining DSSCs with multi–electron catalysts. These multi–electron catalysts must be capable of storing multiple redox equivalents and driving fuel–forming reactions such as water oxidation and CO_2 reduction.

Here we present an overview of energy conversion in natural and artificial photosynthesis. In the first section, the light harvesting, charge separation, and catalytic processes that take place during solar energy conversion in natural photosynthesis are described. In the following artificial photosynthesis section, model molecular systems, specifically electron donor–acceptor assemblies, are used as examples to illustrate the general principles of solar energy conversion by photoinduced charge separation. This is followed by an examination of practical devices, in particular photoelectrochemical cells, for converting solar energy into electricity and chemical fuels. The three key components of light harvesting, charge separation, and catalysis in photosynthesis are then compared between the natural and artificial systems. Photoprotection mechanisms in both systems are also discussed.

Natural Photosynthesis

Nature has implemented a range of photosynthetic systems that reflect the wide variety of habitats photosynthetic organisms can be found in. These systems have some commonalities, however. Here the basic design principles of natural photosynthesis from light harvesting through charge separation to catalysis and photoprotection mechanisms are discussed.

Light Harvesting

Photosynthetic organisms universally exploit antenna systems to absorb light and funnel the excitation energy to the RCs, where the charge separation occurs. This process converts light energy to chemical energy. The use of antenna allows a multitude of pigment molecules to direct light excitation energy to each RC. This architecture increases the number of photons and the range of photon energies that can be directed to a RC to perform charge separation. By increasing the probability that a given RC will produce a charge separation per unit time, antenna enable the rate of RC turnover under ambient sunlight to be matched to the rate of downstream biochemical processes for more efficient biosynthetic function. Furthermore, this arrangement also allows for a degree of control over energy flow in the system (Bailey and Grossman, 2008).

Several major types of photosynthetic antenna exist, including the green sulfur bacterial chlorosome (Pšenčík et al., 2004), cyanobacterial phycobilisomes (Adir, 2005), dinoflagellate peridinin–chlorophyll–protein (Larkum, 1996), the Pcb (*Prochlorococcus* chlorophyll a_2/b binding) protein (Ting et al., 2002), higher plant light-harvesting complex II (LHCII) (Liu et al., 2004), and the purple bacterial light-harvesting complexes

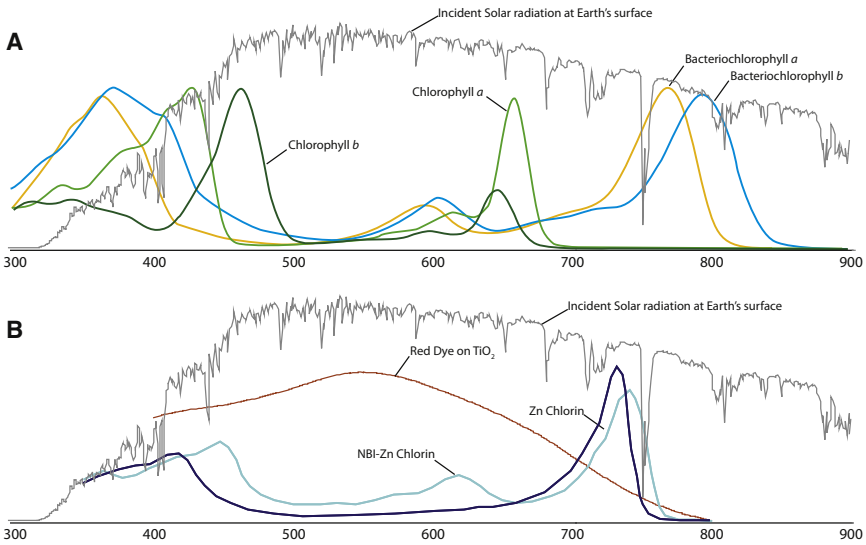

Figure 1. Solar Spectrum Utilization of Natural and Artificial Pigments

(A) Absorption spectra of chlorophylls *a* and *b*, plus bacteriochlorophylls *a* and *b* (in methanol or ethanol) are indicated in color (Blankenship, 2002). (B) Absorption spectra of a TiO_2 thin film sensitized with a Ru-based Red Dye, NBI-Zn-Chlorin and Zn-Chlorin are indicated in color, where the Red Dye has the formula of $RuL_2(NCS)_2\bullet 2TBA$ (L, 2,2′−bipyridyl−4,4′−dicarboxylic acid; TBA, tetrabutylammonium) and NBI represents naphthalene bisimide. The solar spectrum incident on the earth's surface (air mass 1.5, NREL) is indicated in gray in both panels (the spectra of NBI-Zn-Chlorin and Zn-Chlorin are reproduced from Röger et al., [2006]).

1, 2, and 3 (LH1−LH3) (van Grondelle and Novoderezhkin, 2001). Although they are structurally diverse (e.g., the first is a large complex of aggregated pigment molecules, the second and third are soluble pigment-protein complexes, while the last four are intrinsic membrane pigment-protein complexes), which reflects the widely differing environments of the organisms they are found in, each antenna complex performs the function of harvesting light energy in the form of coherent excited-state superpositions referred to as excitons (van Amerongen, 2000; Hu et al., 1998). In spite of gross structural differences, the various antenna complexes use similar principles for light harvesting, made obvious through structural comparison (Cogdell et al., 2008). These features are: highly ordered arrays of pigments, use of pigments competent for transmission of exciton energy via the Förster and Dexter exciton transfer mechanisms (for theory, see van Grondelle (1985, 1994)), and organization of pigments in an energy hierarchy. The Soret, Q_x, and Q_y absorption bands of $\pi \rightarrow \pi^*$ transitions in the chlorin macrocycle of the (bacterio)chlorophyll ((B)chl) pigments are shown in Figure 1A. Here we will discuss the well-studied membrane protein complex consisting of the bacterial reaction center (bRC), in association with LH1 and LH2, as an example. Together these form a photosynthetic unit (PSU), a term used to refer to a RC and its associated antenna that add up to a functional unit incorporating light harvesting through to charge separation.

The purple nonsulfur bacterium *Blastochloris viridis* has only LH1 and a RC, while other purple nonsulfur bacteria such *Rhodobacter* (*Rb.*) *sphaeroides* and *Rhodospirillum* (*Rhs.*) *molischianum* also have LH2, with a membrane organization that has been revealed by atomic force microscopy (Fromme, 2008; Hunter et al., 2009; Sturgis et al., 2009). LH1 and LH2 are transmembrane pigment-protein complexes that form multimeric ring structures. LH1 forms a ring surrounding the RC; the LH2 antenna complexes form smaller rings that surround the LH1 ring in the membrane and are next to other LH2 complexes (Figure 2A).

The crystal structure of LH2 from *Rhodopseudomonas acidophila* at 2.5 Å resolution (McDermott et al., 1995) shows that an LH2 ring is composed of nine monomers (the LH2 ring in *Rhs. molischianum* has only eight monomers; the precise number varies with species). Each monomer is made up of two transmembrane polypeptides: α and β that together noncovalently bind three Bchls, and one carotenoid. The Bchls form two groups of pigments. Two Bchls per monomer are arranged in pairs to form the B850 pigments (B850 meaning a Bchl with an absorption maximum at 850 nm) and the third Bchl is spaced farther apart from other Bchls to form the B800 pigments (Koepke et al., 1996). There is also one spheroidene carotenoid per monomer absorbing in the 450−550 nm range that is bound noncovalently in close contact with a B800 Bchl (Gall et al., 2005). LH1 is also made up of α and β protein monomers that associate to form a ring, in this case a larger ring surrounding the RC. However, different from LH2, each LH1 monomer binds only three chromophores: two Bchls and a carotenoid, with pairs of B875 Bchls adjacent to the carotenoid (Roszak et al., 2003). The proximity of the B850 and B875 Bchls in LH2 and LH1, respectively, produces a strongly exciton-coupled system; each exciton in the B850 ring system is distributed over approximately 4 Bchls (Balzani et al., 2008).

The pigments in a PSU are generally arranged in an "energy hierarchy" (Zinth and Wachtveitl, 2005), with energies decreasing toward the RC. Light energy absorbed by the B800 Bchls and the spheroidine molecules is rapidly transmitted to the B850 Bchls. Excitons in the B850 ring can then be exchanged with other LH2s or with the B875 Bchls in LH1. Exciton energy in the B875 Bchl ring can be transmitted to the "special pair" of Bchls called P870 in the RC (Figure 2A).

Effective exciton energy trapping and transfer in the LH1 and LH2 complexes result from the physical arrangement of the pigments. Exciton transfer is only possible when two excited states are resonant with each other, i.e., two chromophores possessing equivalent energy levels (Ritz et al., 2002). The LH1 complex maximizes this by organizing its B875 Bchls in a large ring. This organization broadens the energy of the excited states, increasing resonance between excited pigments, which in turn increases the rate of transfer. This rate coupled with rapid decay to a lower-lying optically forbidden state produces the rapid one-way transfer of excited state energy between the Bchls. Exciton transfer also couples the higher energy carotenoid pigments to the Bchls. These pigments are very close to each other (~3 Å). Such a close association is necessary because the short lifetime

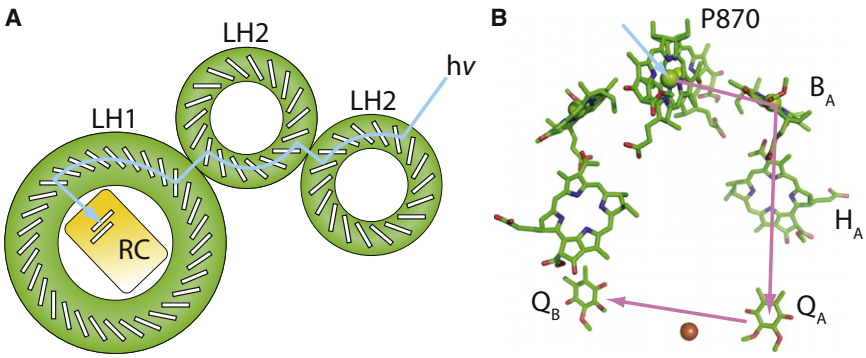

Figure 2. Exciton and Electron Transfer in Bacterial Photosynthesis
(A) A potential path of exciton energy transfer through the bacterial light harvesting system (blue arrow), entering as a photon at an LH2, and traveling though another LH2, then LH1 before arriving at the RC (also denoted with the blue arrow in B). The Bchls of the P870 special pair (RC) and the rings of Bchls in B850 (LH2) and B875 (LH1) are represented by white boxes with black outlines.
(B) The path of electron transfer after a charge separation event at the bacterial reaction center (purple arrows). The electron travels from P870 via accessory Bchl (B_A) to Bpheo (H_A) to the ubiquinone (Q_A). A doubly reduced ubiquinone docked in the Q_B site leaves the reaction center by exchanging with the pool of oxidized quinone in the membrane.

of excited states in carotenoids (10 ps (Larkum, 1996)) would preclude efficient exciton transfer over longer distances.

Transfer of excitation energy between the LH2, LH1, and RC pigments is very fast. Light absorbed by a B800 Bchl in LH2 can be transferred to the B850 ring in 0.7 ps, between B850 Bchls in 100 fs, then to LH1 B875 Bchls in 3 ps. Between LH1 B875 Bchls, it takes 80 fs, and finally to P870 in the RC in 35 ps. This last step is the slowest but this helps prevent back reactions (Fleming and van Grondelle, 1997).

Antenna systems are usually thought of as energy funnels, capturing high energy photons as excitons and funneling them toward an RC, down an energy gradient, presumably to avoid back reactions. This is indeed the case in bacterial photosynthesis under low light conditions, when some bacteria express another antenna complex LH3, which is similar to LH2 but uses B820 Bchls instead of B800 Bchls. In this circumstance, the limited excitation energy is directed to the RCs down an energy gradient. Interestingly, modeling indicates that the funnel effect is not so apparent under typical light conditions when bacteria have predominantly LH1and LH2. The rate of forward and back reactions (both calculated and measured) indicate similar orders of magnitude for each, suggesting a far more even distribution of energy across the antenna system and RCs; despite this, excitons are calculated to be trapped within picoseconds of absorption on average (Ritz et al., 2002).

In addition to the wide array of light-harvesting protein complexes found in nature, a wide array of pigments is also used; some are shown in Figure 1A. Not unexpectedly, the wavelengths that the pigments of antenna systems have evolved to absorb follow a set of rules (Kiang et al., 2007). The first rule that photosynthetic organisms follow is that the absorbance peaks are tuned to the area of the spectrum with the peak photon flux. The RC pigment absorption peak will align with the longest available wavelength within the constraint that the photon energy must be sufficient to drive the necessary (photo)chemistry, e.g., water oxidation and $NADP^+$ reduction in oxygenic photosynthetic organisms or transmembrane proton translocation in anaerobic photosynthetic organisms. Typically, the accessory pigments have another absorption peak at the shortest available wavelengths, given the solar spectrum that passes through the atmosphere. This explains the "green gap" in higher plant pigments, shown in Figure 1A. There is some suggestion that optimal absorption efficiency occurs between 680 nm and 700 nm (Zinth and Wachtveitl, 2005). Many anaerobic photosynthetic bacteria must make do with light that has been filtered by overlaying oxygenic ("green") or other photosynthetic organisms. For example, *B. viridis* can use light beyond 1000 nm with Bchl *b* based antenna (Trissl, 1993). Its RC special pair has a Q_y transition at 960 nm (Zinth and Wachtveitl, 2005). Light of this wavelength has limited energy per photon, limiting the amount of physiological work that can be done once the light has been absorbed by the organism but indicating that useful work can be performed with light from a surprisingly wide section of the solar spectrum.

Charge Separation

Exciton energy present in the antenna system is directed to an RC to convert light energy into chemical energy (the RC can also absorb light directly). The light energy is used to drive the primary charge-separation reaction. RCs are universally transmembrane proteins, vectorially oriented in a lipid bilayer membrane that is exploited as a diffusion barrier to store chemical potential as a proton gradient across that membrane. The goal of the RC is to quickly produce a stable charge separation with minimal wasteful back reactions. A high quantum efficiency can be obtained when all absorbed photons result in a long-lived charge separation ($P^+Q_A^-$). This is achieved through the coordination of energetics, electronic couplings, and reorganization energies (van Brederode et al., 1997). In the bRC, a charge separation over the distance of 25 Å can be achieved in picoseconds (Zinth and Wachtveitl, 2005).

The RCs of the purple bacteria have been intensely studied with regard to kinetics and energy levels. This is because the bRC is easily isolated from its antenna complexes and the pigments in the bRC have well-defined and separated absorption peaks (Zinth and Wachtveitl, 2005). The *B. viridis* RC was the first RC structure to be crystallographically determined; this was achieved in 1987 (Deisenhofer and Michel, 1989; Michel and Deisenhofer, 1987). The RC of purple nonsulfur bacteria (see Figure 2), such as *Rb. sphaeroides* , consists of three polypetides, L, M and H, that bind all the redox-active cofactors. The site of primary charge separation in this RC is made up of two Bchls called P870 that form a "special pair"–so called because they are excitonically coupled though proximity to each other with electronic orbital overlap. In addition to P870, the other pigments are two accessory Bchls (B_A and B_B), two bacteriopheophytins (Bphe, H_A and H_B), and two quinones (Q_A and Q_B). These redox cofactors are arranged in A and B branches with approximate C_2 symmetry, and the A branch does > 99%

of the electron transfer (Figure 2B). This is mainly due to different protein environments around the two branches that modulate the electronic properties of pigments. Factors for the dissimilarity include a greater protein dielectric strength along the A branch that appears to stabilize the charge-separated states (Steffen et al., 1994). Alteration of the pigment hydrogen-bonding patterns generally decreases electron-transfer rates, but some changes can increase the rate, at the expense of resonance with the antenna pigments, with both changes leading to a decrease in quantum efficiency (Zinth and Wachtveitl, 2005).

The RC special pair must be tuned for optimal spectral overlap with the long wavelength absorption band of the antenna (Zinth and Wachtveitl, 2005). This requires the use of appropriate pigments, and the excitonic coupling of the special pair Bchls. The environment of the special pair in the protein is also important: hydrogen bonding modulates the special pair's reduction potential and absorption peaks.

Once the exciton arrives at the RC, it is transferred to the special pair (Hoff and Deisenhofer, 1997). The pigments that surround the excited special pair might be expected to facilitate a very fast back exciton-transfer reaction, returning the special pair to the ground state quickly. In fact, many systems produce an exciton-transfer equilibrium between the RC and the antenna pigments. The RC avoids a reduction in its quantum efficiency and traps excitation energy effectively by a fast and long-lived charge-separation reaction that out-competes other excited state deactivation processes. This is achieved by the formation of $P^+B_a^-$ in 3 ps and the formation $P^+H_A^-$ in 0.9 ps, a total energy drop of 2000 cm^{-1}, sufficient to suppress the back exciton-transfer reaction (Zinth and Wachtveitl, 2005).

Quantum efficiency can also be reduced by the recombination of the initial charge separation states, resulting in the regeneration of the special pair ground state. This will always be a problem for a single electron transfer process because the barriers for the forward and backward reactions are almost always similar (in large part determined by electronic coupling and Franck–Condon factors). Multiple fast forward electron transfers to form the $P^+Q_A^-$ state prevent charge recombination by creating a large distance (25 Å) between the electron donor and acceptor (Zinth and Wachtveitl, 2005).

Once the $P^+Q_A^-$ state has been reached, the charge separation is stable for time scales long enough to enable slower electron and proton transfer events to occur (Zinth and Wachtveitl, 2005). These reactions include $Q_A^- \rightarrow Q_B$ and protonation of the quinone bound at the Q_B site to form the hydroquinone product, both of which occur on a ms time scale that brings all the previous steps into thermal equilibrium. This means that the intermediate states will be populated according to the Boltzmann distribution. The energy of the $P^+Q_A^-$ state must be sufficiently low in comparison with the energies of the intermediates involved in the fast charge-separation reactions and the energy of the special pair excited state to prevent back reactions by thermal equilibration. In *B. viridis*, about half of the photon energy is given up to avoid recombination of the $P^+Q_A^-$ state in order to maintain high quantum efficiency (Table 1).

The RC system in higher plants uses two RCs in series (PSII and PSI) (Golbeck, 2006; Wydrzynski and Satoh, 2005) in what is known as the Z–scheme (Figure 3), each with their own set of antenna pigments to perform work in transporting electrons.

Table 1. Quantum and Energy Efficiencies for Absorbed Photons with Respect to Charge Separation in *B. viridis*, Photosystem II and Dye-Sensitized Solar Cells for Photons at the λ_{max} of Each RC

		Efficiency	
Reaction center	RC λ_{max} (nm)[a]	Quantum[b]	Energy[c]
B. viridis	960	0.96	48% (34%)[d]
Rhs. sphaeroides	870	0.96	44% (37%)[d]
PS II	680	0.92	84% (46%)[e]
DSSC	550	0.90	24% (11.18%)[f]

The numbers for photosynthetic RCs compare only the efficiencies for charge separation in the RC and do not reflect overall solar energy utilization efficiencies.

[a] Absorbtion maximum of pigments in reaction center performing initial charge separation.

[b] Fraction of absorbed photons that result in stable charge separation: *B. viridis* and *Rhs. sphaeroides* (Popovic et al., 1986), PSII from α parameter of 8%, and DSSC (Grätzel, 2005).

[c] Taken as a ratio of the first "stable"charge separated state energy (P^+/Q_A^- or $TiO_2(e^-)/Dye^+$) over the energy of a photon of energy λ_{max}.

[d] The number in parentheses is the efficiency based upon energy stored by charge separation to Q_B using photons at λ_{max} and includes the effect of quantum efficiency.

[e] The number in parentheses is the efficiency based upon energy stored by charge separation between water and Q_B using photons at λ_{max} and includes the effect of quantum efficiency.

[f] The number in parentheses is the overall solar energy conversion efficiency, as determined in (Nazeeruddin et al., 2005).

The movement of the electron down the chain is coupled to proton transport across the membrane, a form of charge storage that is used for energy generation. Using two photosystems allows two visible photons to be used to transport the same electron, applying more energy to generate a greater proton gradient across the membrane within the energetic constraints for water oxidation and $NADP^+$ reduction.

Catalysis

All bRCs couple multi-electron catalysis to single electron photochemistry through double reduction of a quinone to quinol. However, PSII is unique in that it is the only RC able to harness four single electron charge separation events to power the four-electron oxidation of two water molecules to O_2 in the OEC. PSII is the only enzyme known to perform this function and it is able to do so using light energy from the visible spectrum. This requires very precise redox positioning of multiple cofactors. The OEC consists of an inorganic Mn_4Ca cluster and the associated ligating protein. Each charge separation event removes one electron from the OEC via a redox active tyrosine Y_Z in a proton-coupled reaction.

The redox active tyrosine Y_Z is an important component of PSII design. Y_Z is rapidly oxidized by $P680^+$ (~20–200 ns) (Rappaport and Diner, 2008), acting to prevent recombination of the primary charge separation. This couples the much slower oxidation of the OEC to the fast charge separation events occurring at P680. Y_Z is strongly hydrogen bonded to an adjacent histidine. This histdine accepts a proton from Y_Z when Y_Z is oxidized, forming the neutral radical $Y_Z^\bullet$. The oxidized $Y_Z^\bullet$ then acts as a powerful oxidant in turn to advance the oxidation state of the OEC. Oxidation of the OEC reduces $Y_Z^\bullet$ and the proton is returned regenerating Y_Z. This proton coupled electron transfer

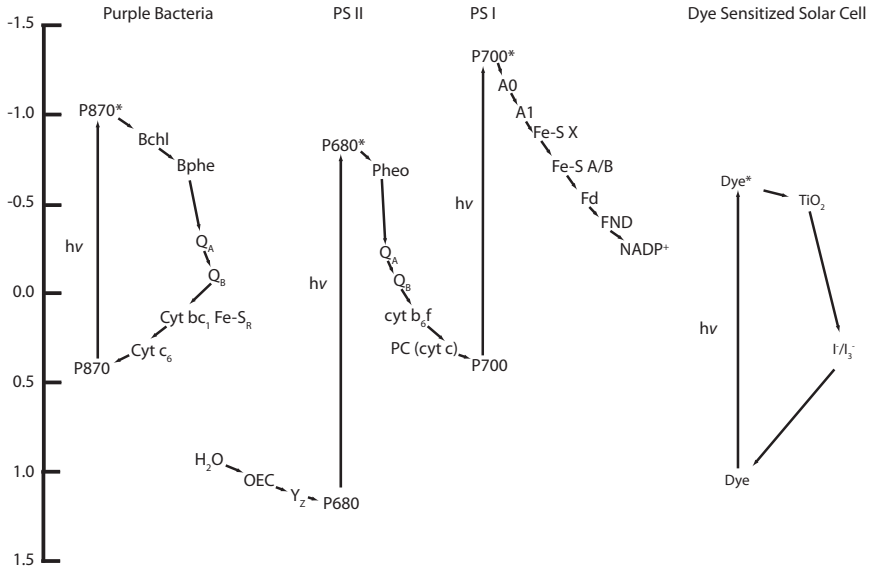

Figure 3. Reduction Potentials in V (versus SHE) in Redox Intermediates in RCs and DSSCs

Energy level diagram of purple bacterial and higher plant (photosystems I and II) reaction centers (Blankenship, 2002; Rappaport and Diner, 2008) in addition to a dye sensitized solar cell using N3 red dye (Grätzel, 2005).

(PCET) reaction adjusts the potential of Y_Z to improve the rate of $P680^+$ reduction and OEC oxidation (Moore et al., 2008).

The Mn ions of the OEC act as a reservoir of oxidizing potential and are also hypothesized to form at least one binding site for substrate water in the catalytic site. The five intermediate oxidation states in the catalytic cycle of the OEC are called S-states, S_n, where n = 0-4. Dark-adapted PSII is predominantly in the S_1 state due to dark deactivations of the higher S-states back to the S_1 state. However, all of the S-states are long lived enough to persist between sequential oxidations that occur at rates on the order of μs–ms under saturating light. On reaching S_3, the next photochemical turnover poises the system at its rate-limiting step; oxidation of the S_3 state by $Y_Z^{\bullet}$ produces the S_4 state, which spontaneously decays rapidly to the S_0 state together with the formation of O_2. The four flashes required to complete the cycle result in a characteristic period four oscillation of oxygen release under a series of actinic flashes.

The OEC catalyzes the formation of an O=O bond. It is the only enzyme known that can do so with two water molecules as substrates. The precise mechanism is not known, but current hypotheses invoke either a Mn^V=O or Mn^{IV}–$O^{\bullet}$ species undergoing nucleophilic attack by a water molecule (Brudvig, 2008; McEvoy and Brudvig, 2006).

The operating potentials of the intermediates in the catalytic cycle of the OEC are estimated to be approximately 1.11 V for S_2/S_1, 1.14 V for S_3/S_2, 1.2 V for $S_3Y_Z^{\bullet}/S_3Y_Z$, and 1.07 V for S_4/S_0 versus SHE (Rappaport and Diner, 2008). These potentials are remarkably close to each other, a phenomenon called redox leveling that is not typically observed for sequential oxidations of a single redox center. PCET is believed to facilitate redox leveling in the OEC and allows for sequential electron removal without coming up against insurmountable energetic barriers (McEvoy and Brudvig, 2006; Rappaport and Lavergne, 2001).

The OEC uses Mn as the catalytic metal. Mn is able to increase the availability of OH^- and O^{2-} species by lowering the pK_a of bound water from 10.5 to 0 on oxidation from Mn^{II} to Mn^{III} and even lowering the pKa of Mn^{IV}-bound OH^- to 0, in addition to stabilizing these ligands by virtue of unfilled d–orbitals (Armstrong, 2008).

Indeed, the Mn and Ca ions in the OEC are connected by μ–oxo bonds (Pushkar et al., 2007; Yano et al., 2006). In addition to its rich redox chemistry, Mn is the twelfth most abundant element in the earth's crust, and the third most abundant transition metal, with high bioavailability in the form of the very soluble Mn(II) cation. All of these factors make it a good choice for organisms to exploit in demanding redox applications (Armstrong, 2008).

The lowest oxidation state of Mn in the catalytic cycle of the OEC is Mn^{III} (the S_0 state is $Mn^{III}{}_3Mn^{IV}$), avoiding any potential problem with the lability of Mn^{II} (Armstrong, 2008). This is important because the process of water oxidation is much slower than the charge-separation reactions. The maximum rate that PSII can produce O_2 is around 50 s^{-1}, limited by quinone diffusion into and out of the Q_B site. In reality, however, charge separation events may not be happening so quickly; each antenna Chl absorbs less than one photon per second, so the water oxidation reaction intermediates must be stable for some time.

The OEC is almost exclusively ligated by the D1 protein, and the D1 protein also ligates the Chl species P680. Even given approximately 2.5 Gya of evolution (Bekker et al., 2004), the extreme oxidations that take place in this system result in damage that must be repaired regularly by replacing the D1 protein. This replacement occurs on the order of every 20 min (Vasilikiotis and Melis, 1994).

Photoprotection

Natural photosynthesis (especially oxygenic photosynthesis) is optimized for function at low light and is strongly saturated under the midday sun (Demmig-Adams et al., 2006). Under high light conditions, charge recombination can occur in the RCs due to extended intermediate lifetimes in over-reduced systems; e.g., if Q_A^- cannot transfer an electron to Q_B because the quinone pool is fully reduced, then charge recombination will be enhanced. This can lead to triplet state Chls that are able to react with O_2 to create highly reactive and destructive singlet O_2 molecules that are potentially fatal to the organism.

Photosynthetic organisms employ several protective mechanisms to survive high light conditions (Demmig-Adams et al., 2006). One simple way that photodamage can be minimized is by decreasing the antenna size. For example, *Rb. sphaeroides* produces less LH2 when it is grown under high light conditions in comparison with lower light conditions. Carotenoids also play important photoprotective roles. Chl triplet energy transfer to fast relaxing carotenoids can quench triplet state Chls before they react to form singlet O_2. In addition, "secondary" electron transfer involving carotenoids produces a dissipative cycle in PSII (Frank and Brudvig, 2004).

To deal with transient light intensity variations, faster mechanisms are required. When transient excessive light conditions occur, antenna systems can induce mechanisms to dissipate absorbed light energy as heat, rather than funnel excitons to RCs where they can be used for charge separation (Chow et al., 2005). Antenna complexes are able to dissipate light excitation energy through photochemical (fluorescence) and nonphotochemical quenching (NPQ) processes. Although the molecular mechanisms are still not well understood, they always involve the quenching of singlet excited chlorophylls (Müller et al., 2001) with the energy dissipated to heat.

Artificial Photosynthesis

In this section, the essential components and basic principles of artificial photosynthesis are described using donor–acceptor model systems as examples. Photoinduced charge separation events in dye-sensitized solar cells (DSSCs) are then compared with those in the model systems. The design of DSSC–based photoelectrochemical synthesis cells for solar fuel generation is then discussed. A brief introduction to photoprotection in artificial photosynthetic systems is also included.

Artificial Photosynthetic Model Systems

By mimicking the natural system, an artificial photosynthetic assembly can be prepared consisting of a light harvesting unit, a RC for charge separation, and catalysts for multi–electron fuel–forming reactions. These components should be suitably coupled and organized in the dimensions of time, energy, and space (Balzani et al., 2008). This section focuses on donor–acceptor assemblies as artificial photosynthetic model systems.

Light Harvesting Units. In an artificial system, light harvesting can be achieved by using a single "reaction center" chromophore or by the excitation of a light–absorbing antenna array followed by the energy–transfer sensitization of an RC (Alstrum-Acevedo et al., 2005). Among the light–harvesting chromophores, porphyrins and phthalocyanines are closely related to chlorophyll derivatives. Metal coordination compounds, which exhibit metal–to–ligand charge transfer (MLCT) at relatively low energy, have been widely employed as photosensitizers (Huynh et al., 2005). Early work in designing molecular model systems focused on light absorption and excited–state electron transfer involving the $\pi \rightarrow \pi^*$ transition of porphyrins and the MLCT of $[Ru(bpy)_3]^{2+}$ (bpy = 2,2′–bipyridine) (Meyer, 1989; Wasielewski, 1992; Balzani et al., 2006).

Nature has developed highly complex light–harvesting systems to utilize the full solar spectrum. Artificial systems can be designed with enhanced light–harvesting capacity and efficiency. For example, Würthner and coworkers prepared a bichromophoric assembly consisting of blue naphthalene bisimide (NBI) dyes at the periphery of aggregated zinc chlorines (Röger et al., 2006). As model compounds for Bchl *c*, zinc chlorins are very efficient in harvesting blue and red light, but not the significant green region (Figure 1B). The artificial bichromophoric assembly absorbs green light and demonstrates efficient energy transfer from the NBI dyes to the zinc chlorines (Figure 1B) (Röger et al., 2006). Wasielewski and coworkers developed a perylene–based green chromophore analogous to chlorophyll *a* in photophysical and redox properties (Lukas et al., 2002). Unlike chlorophyll *a*, the chromophore can be easily functionalized and incorporated into a wide variety of biomimetic electron donor–acceptor systems (Lukas et al., 2002). They also demonstrated that supramolecular light–harvesting arrays can be constructed by self–assembling chromophore building blocks in solution and on surfaces (Ahrens et al., 2004; Kelley et al., 2008).

Antenna systems are capable of collecting light and transferring energy in an efficient and direct way. When a RC is coupled to an antenna array, a large number of antenna chromophores surrounding the RC absorb incident photons. The resulting excited states then transfer electronic energy to the RC before undergoing radiative or nonradiative deactivation. Highly branched tree–like dendrimers have been widely employed as antenna systems. The convergent and/or divergent synthesis of dendrimers allows the assembly of a large number of chromophores in close proximity, where various functional groups can easily interact with one another (Balzani et al., 2008). Most of the known artificial antenna systems have been constructed using multiporphyrin arrays (Nakamura et al., 2007), porphyrin dendrimers (Imahori, 2004), or dendrimers based on metal complexes and organic molecules (Nantalaksakul et al., 2006; Serroni et al., 2003). It should be pointed out that the incorporation of antenna chromophores in artificial systems may not be beneficial if the antenna array and the RC are not properly coupled in the dimensions of time, energy, and space. In fact, reducing the antenna size has been shown to improve photosynthetic solar energy conversion efficiency in natural systems (Melis, 2009).

Charge Separation. In natural photosynthesis, solar energy is captured and stored via photoinduced charge separation reactions. Model systems, such as donor–acceptor assemblies, have been designed and synthesized, mimicking the electron donors and acceptors found in photosynthetic proteins (Figure 4). Important considerations for donor–acceptor assemblies include the directionality of electron transfer, electronic coupling between the donor/acceptor and the chromophore, charge separation, and the storage of redox equivalents for multi–electron reactions.

The minimum model for a donor–acceptor assembly is a molecular dyad, such as the porphyrin–quinone (P–Q) system. In the P–Q system, the covalently linked porphyrin and quinone function as the electron–donor chromophore and electron acceptor, respectively. Such a simple model system can mimic certain aspects of natural photosynthesis and help elucidate basic photochemical principles (Gust and Moore, 1989). However, the P–Q system is unable to maintain an energetic charge–separated $P^{\bullet+}$–$Q^{\bullet-}$ state long enough to allow the extraction of useful work from it. Typically, the $P^{\bullet+}$–$Q^{\bullet-}$ state survives only a few hundred picoseconds or less in solution because the geometric factors that facilitate efficient photoinduced charge separation also favor rapid charge recombination to the ground state (Gust and Moore, 1989).

Recent studies on some dyad systems have provided important examples of alternative designs for efficient artificial photosynthesis (Song et al., 2009; Herriman, 2004; Schuster et al., 2004). More importantly, studying the relatively simple molecular dyads has inspired the development of more complex model systems. Figure 4A shows the structure of a molecular triad constructed by using a porphyrin (P) photosensitizer linked to a carotenoid (Car) electron donor on one side and a quinone (Q)

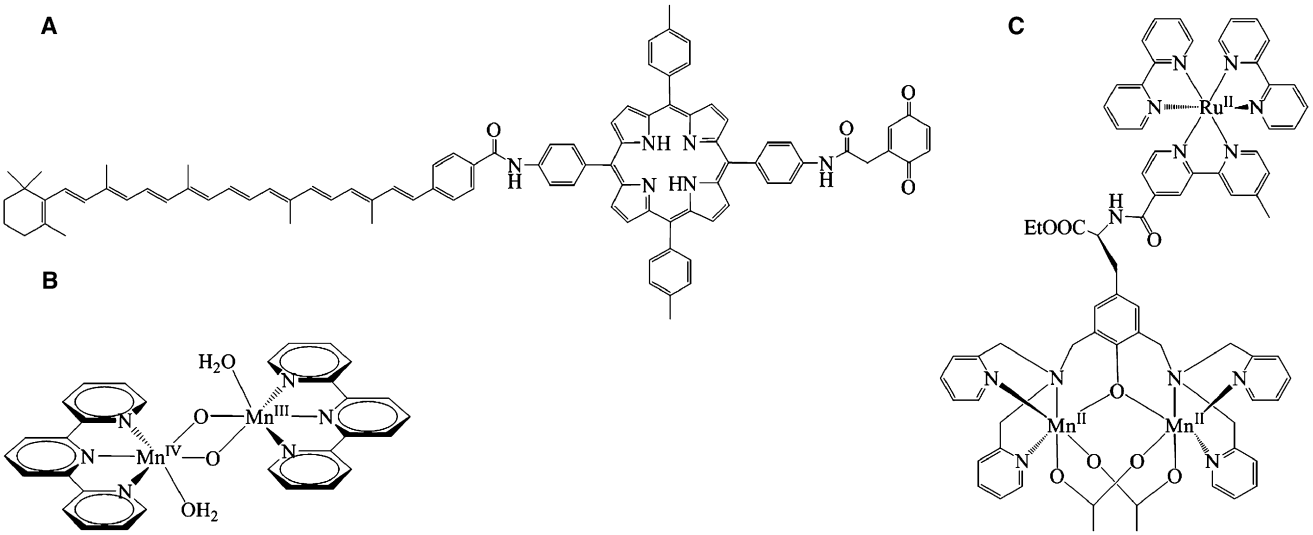

Figure 4. Structures of Biomimetic Compounds
(A) A carotenoid–porphyrin–quinone molecular triad, (B) a dinuclear di-μ-oxo Mn(III,IV) water-oxidation catalyst, and (C) a Ru–Mn(II,II) complex.

electron acceptor on the other side (Moore et al., 1984). In this Car–P–Q triad, photoexcitation of the porphyrin yields the first excited singlet state, Car–^{1}P*–Q (Figure 5A). The excited state decays via a sequential, two–step, electron–transfer process, leading to the formation of a Car$^{\bullet+}$–P–Q$^{\bullet-}$ charge–separated state with a lifetime on the μs timescale (Moore et al., 1984). Charge recombination is significantly slowed because of the interposition of a neutral porphyrin between the widely separated ions (Moore et al., 1984). This triad approach mimics the strategy used in natural RCs in which multistep electron transfers occur through a series of donors and acceptors. Other complex assemblies, such as nanostructured porphyrin–fullerene architectures (Fukuzumi and Kojima, 2008; Imahori et al., 2003), have attracted as much attention as donor–acceptor model systems, as summarized in recent reviews (Balzani et al., 2008).

The ability to optimize charge separation over charge recombination, thereby creating long lived charge–separated states, is essential for the development of efficient artificial photosynthetic systems. In donor–acceptor assemblies, the electron transfer rate is a function of donor–acceptor orientation, the solvent, the intervening linkage or other medium, and the temperature. Wiberg et al. (2007) investigated how the donor–acceptor distances and donor–bridge energy gaps influence the rates of charge separation and charge recombination differently in a donor–bridge–acceptor model system. They show that the exponential distance dependence increases slightly for charge recombination in comparison with that for charge separation. They also show that the effect of the tunneling barrier height is different for charge separation and charge recombination and that the difference is highly dependent on the electron acceptor.

Multi–Electron Catalysts. In an artificial photosynthetic assembly, the light–harvesting unit and the RC must be coupled to water–splitting catalysts or CO_2–reduction catalysts to produce chemical fuels (Lewis and Nocera, 2006; Lubitz et al., 2008). Transition–metal complexes are known for their capacity to store multiple redox equivalents. A variety of homogeneous water–oxidation catalysts (Cady et al., 2008; Yagi et al., 2009) have been developed containing transition metals including

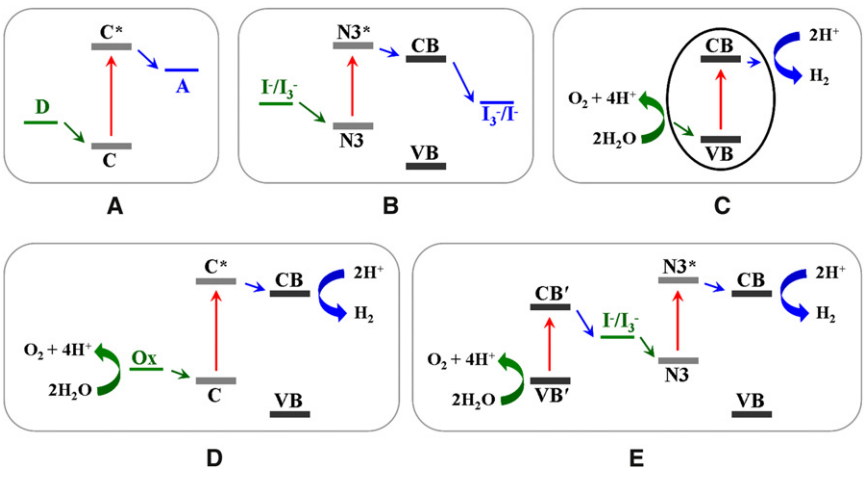

Figure 5. Photoinduced Electron Transfer in Different Artificial Systems
(A) A molecular triad, (B) a DSSC, (C) a semiconductor photocatalyst, (D) a DSSC coupled to a water–oxidation catalyst, and (E) a tandem water–splitting cell. Energies are not to scale.
CB and VB, conduction band and valence band; D, electron donor; C, chromophore; C*, photoexcited chromophore; A, electron acceptor; N3 and N3*, ground state and excited state of the Ru–based N3 dye; Ox, water–oxidation catalyst; and CB′ and VB′, conduction band and valence band of a narrow bandgap semiconductor.

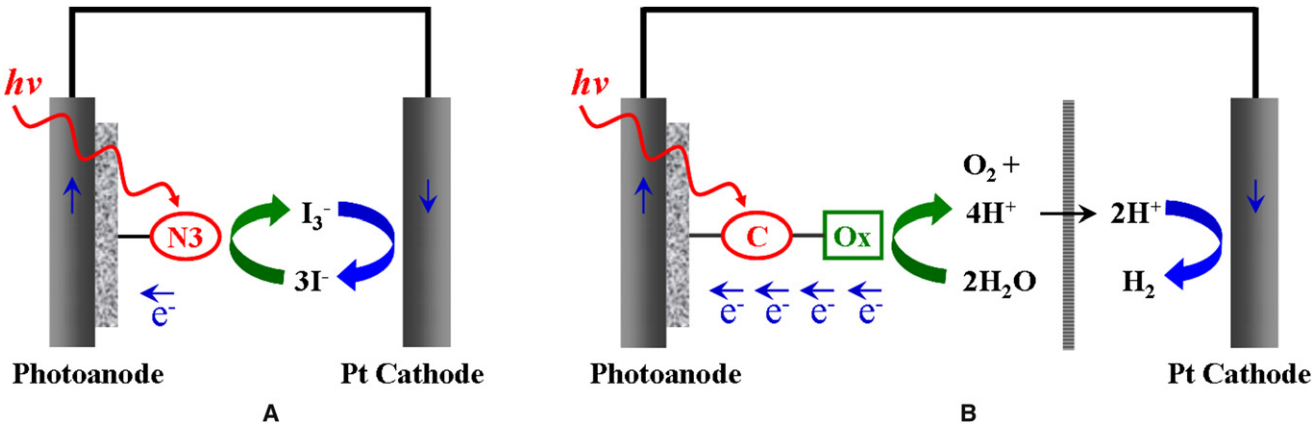

Figure 6. Schematic Representations of Photoelectrochemical Cells
(A) A DSSC and (B) a DSSC coupled to a water–oxidation catalyst. See Figures 5B and 5D for corresponding energy diagrams.
N3, ruthenium dye; C, chromophore; and Ox, water–oxidation catalyst.

Ru (Concepcion et al., 2008; Deng et al., 2008; Gersten et al., 1982; Liu et al., 2008; Sens et al., 2004; Yagi et al., 1997), Mn (Brimblecombe et al., 2008; Chen et al., 2004; Limburg et al., 1999, 2001; Poulsen et al., 2005), and Ir (Hull et al., 2009; McDaniel et al., 2008). Complexes of Ru, Re, Co, and Ni are molecular catalysts capable of mediating electron transfer in the photochemical reduction of CO_2 (Fujita, 1999; Fujita and Muckerman, 2008).

The water oxidation half reaction requires the accumulation of four oxidizing equivalents according to the following reaction:

$$2H_2O + 4h\nu \rightarrow O_2 + 4H^+ + 4e^-.$$

The blue dimer, *cis*,*cis*–$[(bpy)_2(H_2O)Ru^{III}ORu^{III}(H_2O)(bpy)_2]^{4+}$, was the first synthetic water–oxidation catalyst (Gersten et al., 1982). In water oxidation catalyzed by the blue dimer, both electrons and protons are transferred, avoiding charge buildup and allowing for the accumulation of multiple oxidative equivalents at the Ru–O–Ru core (Liu et al., 2008). In the presence of a primary oxidant (such as Ce^{4+}), stepwise e^-/H^+ loss leads to the higher oxidation states $Ru^{V}ORu^{IV}$ and $Ru^{V}ORu^{V}$, both that can oxidize water to oxygen (Liu et al., 2008).

In nature, the production of O_2 through oxidation of water is catalyzed by a Mn_4Ca bioinorganic core in the OEC of PSII (Brudvig, 2008; McEvoy and Brudvig, 2006; Sproviero et al., 2008a, 2008b; Yachandra et al., 1996). As of today, there is still a debate regarding the exact structure and mechanism of water oxidation mediated by the OEC. Bioinspired manganese complexes have been developed as water–oxidation catalysts, including the dinuclear di–μ–oxo manganese complex $[H_2O(terpy)Mn^{III}(\mu\text{–}O)_2Mn^{IV}(terpy)H_2O](NO_3)_3$ (Figure 4B) (terpy = 2,2′:6′2″–terpyridine) developed by Brudvig, Crabtree, and coworkers (Limburg et al., 1999, 2001). The Mn(III,IV) dimer is capable of oxidizing water when activated with a primary oxidant. It is thought to be biomimetic, since some of its structural and mechanistic features are similar to those of the OEC. The catalytic mechanism of water oxidation based on the Mn(III,IV) dimer is thought to involve the formation of a high–valent Mn^{V} = O or Mn^{IV}–O• species (Mullins and Pecoraro, 2008; Tagore et al., 2008). The oxyl radical is susceptible to nucleophilic attack by a water molecule, forming a hydroperoxo intermediate that rapidly decomposes into O_2 upon deprotonation.

An important approach to building complete artificial photosynthesis systems is to develop small, functional building blocks that can be assembled into large integrated structures (Wasielewski, 2006). Coupling single–photon charge separation with multi–electron redox processes remains a major challenge for artificial photosynthesis. Following the principles derived from PSII, Hammarström, Styring, and coworkers have designed and synthesized donor–acceptor assemblies aimed at achieving light–driven water oxidation (Sun et al., 2001). They prepared supramolecular complexes analogous to the redox components on the donor side of PSII. For instance, the light–harvesting $[Ru(bpy)_3]^{2+}$ moiety was used as the replacement for P680; Mn complexes, such as a Mn(II,II) dimer (Figure 4C), were incorporated in the assemblies to mimic the OEC (Abrahamsson et al., 2002; Lomoth et al., 2006). Light-induced accumulative electron transfer from the Mn(II,II) dimer to the photooxidized Ru center resulted in the formation of a Mn(III,IV) complex (Hammarström and Styring, 2008; Huang et al., 2002). The researchers also introduced a tyrosine link between the Ru center and the Mn dimer. It was suggested that the incorporation of an intervening redox active link (such as tyrosine) might be crucial to the multistep electron transfer from the Mn cluster to the Ru center, as in PSII (Sun et al., 2001).

Photoelectrochemical Cells

For an efficient artificial architecture, a membrane is usually needed to spatially separate oxidative and reductive species, as occurs in natural photosynthesis. The transfer of electrons across the photosynthetic membranes drives chemical reactions and can also produce electricity. Similarly, electricity can be generated from light by transporting photoexcited electrons between the front and the rear contacts of a solar cell (Markvart, 2000). Photoelectrochemical cells (e.g., DSSCs) utilize this principle to convert solar energy into electricity (Figure 6).

DSSCs were first developed by Grätzel and coworkers as promising alternatives to expensive solid–state photovoltaic devices (Grätzel, 2001, 2005; O'Regan and Grätzel, 1991). They are relatively inexpensive and efficient artificial devices for solar energy conversion. A solar conversion efficiency of

11.18% has been achieved using $[RuL_2(NCS)_2]^{2+}$ (L = 2,2′−bipyridyl−4,4′−dicarboxylic acid), named the N3 or Red dye, in a DSSC (Nazeeruddin et al., 2005). A DSSC consists of a dye−sensitized photoanode, a redox mediator, and a Pt counter electrode. The photoanode is typically a mesoscopic TiO_2 thin film placed in contact with an electrolyte that contains the I_3^-/I^- redox mediator. Following photoexcitation of the dye molecule, an electron is rapidly injected into the conduction band (CB) of TiO_2 nanoparticles (NPs). The injected electron then diffuses through the TiO_2 NP network to be collected as electricity (Figures 3, 5, and 6).

In this section, light harvesting and photoinduced charge separation in DSSCs are compared with those in donor−acceptor systems. The design of photoelectrochemical synthesis cells is also discussed, in which DSSCs are coupled with catalysts for solar fuel generation by water splitting.

Light Harvesting. In a DSSC, light harvesting involves the MLCT transition of the dye molecules, usually polypyridyl Ru complexes, attached to a mesoscopic TiO_2 thin film. A TiO_2 thin film sensitized with the polypyridyl Ru complexes strongly absorbs visible light with a maximum absorbance around 550 nm (Figure 1B). It has been shown that the dye structure can be tuned to improve the molar extinction coefficient and light−harvesting capacity (Gao et al., 2008; Kuang et al., 2006).

The porous, nanostructured TiO_2 film possesses a very high surface roughness and small particle sizes (~20 nm) that allow for efficient light harvesting. A monolayer of dye molecules on a flat TiO_2 surface can only absorb a very small fraction of the incident light because one molecule occupies an area much larger than its optical cross-section for light capture (Grätzel, 2005). In a DSSC, the incident light crosses hundreds of adsorbed dye molecules when it penetrates the sensitized mesoporous TiO_2 film. This enhanced light absorption is similar to that in green leaves, in which light harvesting by chlorophyll is enhanced in stacked thylakoid vesicles (Grätzel, 2005). Furthermore, larger TiO_2 particles (200−400 nm) are usually incorporated in the TiO_2 film in a DSSC to enhance light harvesting in the red or near−infrared region (Hamann et al., 2008).

Charge Separation. A DSSC operates under the same energy conversion model as those of donor−acceptor assemblies. In fact, porphyrin−fullerene donor−acceptor assemblies have been utilized as molecular photovoltaic devices (Imahori and Fukuzumi, 2004). In a molecular triad (Figure 5A), the chromophore (C) absorbs light and initiates charge separation; stabilization of electronic charge separation can be achieved by electron transfer from the electron donor to the electron acceptor. In a DSSC (Figure 5B), the photoexcitation of an electron from the dye molecule (e.g., N3) is followed by the heterogeneous electron injection from the dye to the conduction band (CB) of TiO_2. The oxidized dye molecule is regenerated by electron donation from I^- in the electrolyte. Triiodide (I_3^-), the oxidized product of I^-, is in turn reduced at the Pt counter electrode by electrons passed through the external load. Thus, photogenerated electrons are collected in the external circuit and I_3^- is reduced on the Pt cathode; I^-/I_3^- serves as the redox mediator and no net chemical transformation occurs in the DSSC.

The solar cell efficiency depends on light harvesting, interfacial charge transfer from the dye molecules to TiO_2 (Ardo and Meyer, 2009; Meyer, 2005), and subsequent processes. In DSSCs, radiative or radiation-less deactivation channels include: (1) decay of the excited dye molecule before it injects an electron, (2) recombination of the injected electron with the oxidized dye before the oxidized dye is reduced by iodide, and (3) interception of an electron from the photoanode by the redox mediator before the electron is collected.

Although the decay of the excited dye molecule is very rapid, dye sensitizers have been developed to achieve interfacial electron injection in the pico− or femtosecond time range, achieving quantum yields of charge injection generally exceeding 90% (Grätzel, 2005). Such sensitizers are usually anchored to TiO_2 surfaces through functional groups such as carboxylate, hydroxamate, or phosphonate moieties (Grätzel, 2005). These anchor groups form strong coordinative bonds with surface Ti ions and also enhance electronic coupling between lowest unoccupied molecular orbital (LUMO) of the dye sensitizer with the TiO_2 CB (Grätzel, 2005).

The back reaction of the injected electrons with the oxidized dye in a DSSC is retarded for several reasons, including the small electronic coupling, a large driving force, and small reorganization energy (Grätzel, 2005). The small electronic coupling originates from the small electronic overlap between the TiO_2 CB and the Ru *d* orbital involved in back reaction, and the spatial contraction of the *d* orbital wave function upon oxidation of Ru(II) to Ru(III) (Grätzel, 2005).

In a DSSC, the interception of injected electrons by the redox mediator can be reduced by the addition of surface passivators, such as *tert*−butyl pyridine and guanidinium ion to the electrolyte that block access to exposed TiO_2 surfaces. It has been shown that the presence of guanidinium ion can significantly reduce the recombination rate of photoinduced electrons with I_3^- and lead to a downward shift of the TiO_2 CB (Kopidakis et al., 2006). The collective effect results in the overall improvement in the open−circuit voltage of the DSSC. In addition, O'Regan et al. (2009) demonstrated that the dye structure can influence iodine complexation and, therefore, charge recombination as well as the open−circuit voltage.

Photoelectrochemical Synthesis Cells. As a semiconductor, TiO_2 can be activated by UV light and function as a photocatalyst. Upon activation, an electron is excited to the TiO_2 CB, leaving a positively charged hole in the valence band (VB) (Linsebigler et al., 1995). Theoretically, photocatalytic water splitting can occur on the TiO_2 surface because the CB electrons and VB holes are energetic enough for water reduction and oxidation, respectively (Figure 5C) (Grätzel, 2001; Linsebigler et al., 1995). Fujishima and Honda (1972) have demonstrated the photolysis of water on TiO_2 in the presence of a small external bias. However, this process occurs with extremely low efficiency due to the dominating electron−hole recombination that prohibits the accumulation of multiple oxidizing equivalents in the TiO_2 VB for water oxidation. In addition, the activation of pure TiO_2 requires UV light, which accounts for less than 5% of the natural solar spectrum.

Nevertheless, TiO_2 materials have been widely employed in artificial photosynthesis research (Chen et al., 2009; Reisner et al., 2009). For example, a porphyrin−based bio-inspired construct was assembled on TiO_2 to mimic the proton-coupled electron transfer between $P680^{\bullet+}$ and the Tyr_Z−His190 pair of

PSII (Moore et al., 2008). Because the electrons in the TiO_2 CB are capable of reducing protons to molecular hydrogen, the use of TiO_2 as a robust solid–state support for molecular and supramolecular assemblies could facilitate the development of practical photosynthetic devices for high–efficiency solar water splitting.

As mentioned earlier, a molecular triad can be coupled to multi–electron catalysts to build a complete artificial photosynthetic assembly. Based on this understanding, a photoelectrochemical synthesis cell (Figures 5D and 6B) can be constructed for solar-water splitting by incorporating a water–oxidation catalyst in a DSSC. Recently, Youngblood et al. (2009) prepared an overall water-splitting system by coupling a hydrated iridium oxide nanoparticle, a heterogeneous water–oxidation catalyst, to a DSSC. In this photoelectrochemical synthesis cell, the water–oxidation catalyst is activated by a polypyridyl Ru dye that serves as both a photosensitizer and a molecular bridge. The system demonstrated visible–light water splitting (Youngblood et al., 2009).

Tandem cells featuring a Z–scheme have been proposed as working devices for overall photocatalytic water splitting. In a tandem cell, two photoelectrodes having different bandgaps are superimposed and coupled to a dark counter electrode (Figure 5E) (Cesar et al., 2006; Duret and Grätzel, 2005; Kay et al., 2006; Maeda et al., 2010). The two superimposed photoelectrodes should absorb complementary parts of the solar spectrum. While the electrons in the TiO_2 CB are collected for H_2 production, a narrow bandgap semiconductor, such as WO_3 and α–Fe_2O_3, would serve as the O_2–evolving photoanode.

Artificial Photoprotection

Moore and coworkers prepared an artificial light–harvesting dyad as a model for excess energy dissipation in oxygenic photosynthesis (Berera et al., 2006). The researchers studied a model system made up of a zinc phthalocyanine molecule covalently linked to a carotenoid with conjugated C=C bonds, in which the carotenoid acts as an acceptor of phthalocyanine excitation energy (Berera et al., 2006). In the artificial dyad, quenching proceeds through energy transfer from the excited phthalocyanine to the optically forbidden S_1 state of the carotenoid, coupled to an intramolecular charge–transfer state (Berera et al., 2006). It was also shown that the conjugation length of the carotenoid is critical to the quenching process. In a different study, the researchers demonstrated that a compact architecture consisting of carotenoids and tetrapyrroles closely mimics light–harvesting and photoprotective functions in the natural photosynthesis (Kodis et al., 2004).

Moore and coworkers also prepared a molecular pentad consisting of two light–gathering antennas, a porphyrin electron donor, a fullerene electron acceptor, and a photochromic control moiety (Straight et al., 2008). The molecule mimics the nonphotochemical quenching mechanism for photoprotection found in plants by modifying its function according to the level of environmental light. Specifically, the molecule undergoes photoinduced electron transfer with a quantum yield of 82% when the light intensity is low. As the light intensity increases, the photochrome photoisomerizes, leading to quenching of the porphyrin excited state and reducing the quantum yield to as low as 27% (Straight et al., 2008).

Comparison of Natural and Artificial Systems

There are many similarities between the natural and artificial systems. Light harvesting, charge separation, and catalysis are the key components for both systems, although multi–electron catalysis does not occur in a DSSC. Basic structural similarities are to be expected, given the mimicry that is intended in many of the artificial systems (compare the redox active components in Figure 2B and the acceptor/donors in Figure 4A). There are functional similarities too, such that all of the redox chemistry takes place in a per-electron fashion. Table 1 shows that the per-photon probability of charge separation (quantum efficiencies) of each system is also close. Additionally, there is an obvious similarity between P870 of purple photosynthetic bacteria and DSSCs in terms of pigment ground and excited state energy level difference and the resulting cyclic electron transport (Figure 3).

However, there are also many areas where the natural and artificial systems differ. For example, the structural differences in natural and artificial systems are large. The natural system RCs are embedded in a membrane that simultaneously acts as a pathway for electrons and a barrier for proton diffusion. In photoelectrochemical cells, the electrons are transported through the supporting electrodes and protons diffuse freely. The components of purple bacterial photosynthesis are self assembling while current artificial systems need more guidance. The following sections describe the similarities and differences between natural and artificial systems in light harvesting, charge separation, and catalysis.

Light Harvesting

As seen in Figure 1, natural photosynthesis and DSSCs both exploit pigments to harvest solar energy. A difference between the two types of systems is that natural photosynthesis uses several different pigments to absorb a range of the solar spectrum available in an organism's environment (e.g., Chl *a* and *b* in tandem as in higher plants), whereas DSSCs generally use one type of pigment with a very broad absorption spectrum to exploit the majority of the solar spectrum (compare Figures 1 A and 1B). This is in line with the aim for a solar device to absorb all of the solar radiation to maximize the output of the device. Constructing a multilayer cell with different dyes in each layer allows different components of the solar radiation can be harvested in separate sections of an overall device, similar to an ecosystem with several photosynthetic organisms absorbing light at increasingly lower light qualities down the vertical axis (rain forest or ocean, for example; see the λ_{max} column in Table 1). A note of caution is required, however; due to selection pressure, natural antenna systems are able to absorb so much light that under full sunlight most of it cannot be used for charge separation. This can also lead to shading of catalytic centers not located on the surface of the system. It is well known that limiting antenna size in mass culture of photosynthetic organisms leads to improved radiation-to-product conversion ratios in natural systems (Melis, 2009). The possibility of such an effect in large artificial arrays should also be kept in mind.

Current approaches pair one excitable dye with one RC in DSSCs, but dendrimer–based antenna have been developed to enhance light harvesting and energy transfer in artificial systems. As discussed earlier in this context, efficient light harvesting is achieved by arranging a large number of antenna

chromophores surrounding an RC. The dendrimer–based approach for artificial photosynthetic systems is closer to the natural system's design of antenna complexes.

Charge Separation

The initiation of electron transport is slightly different in natural and artificial systems. The natural PSII complex generates a charge-separated state between pheophytin and Chl molecules within picoseconds after the RC reaches its initial excited state. Then two further electron-transfer steps stabilize the charge separation by reducing a quinone and oxidizing Y_Z before finally oxidizing the Mn_4Ca water-oxidation catalyst. The use of several intermediates and rapid electron transfer down an energy gradient minimizes back reactions, thus increasing efficiency.

In a DSSC, the initial charge-separated state lacks these multiple intermediates. Once the dye injects an electron into the TiO_2 CB, rapid electron transfer from the I^-/I_3^- redox couple to the oxidized dye stabilizes the separation, reducing the likelihood of immediate recombination. The injected electron then needs to avoid recombination with I_3^- at other sites on its diffusion pathway to the anode of the cell.

In a DSSC, the important functions of TiO_2 include supporting the photosensitizer, and collecting and conducting charges. An advantage of using a semiconductor layer rather than a phospholipid membrane, as in natural photosynthesis, is that the TiO_2 film is extremely stable and allows fast electron transport (Grätzel, 2005). In comparison with the TiO_2 film, the charge transfer across the photosynthetic membrane is much slower. In addition, nature sacrifices more than half of the absorbed photon energy to drive the transmembrane redox processes. In the case of the TiO_2 film in a DSSC, only about 50–100 meV of driving force is needed for the electron injection process at the semiconductor/photosensitizer interface (Grätzel, 2005). The efficiencies of charge separation are considered in Table 1 in the energy efficiency column. The bracketed numbers indicate overall efficiency and show that while natural systems might not be optimized for efficient solar fuel production, they are quite efficient for energy conversion in charge separation (34%–46%).

Catalysis

Cheap and abundant Mn is perhaps the ideal metal to be used in a photocatalyst for water oxidation—indeed it is nature's choice. In fact, it seems that nature is restricted to Mn, as no other water–oxidation catalyst has been found apart from PSII. Artificial approaches are not bound by this limitation, however, and it is possible (but more expensive) to use alternate chemistries such as those offered by Ru (blue dimer [Gersten et al., 1982]) and Ir (IrO_2 or Ir–Cp* catalysts [Hull et al., 2009]). The catalyst should be robust and not require repair every 20 min as in the natural system. The ability to bind and stabilize intermediates for relatively long time frames is also important, underlying the need for slow ligand exchanging metals or encapsulation strategies. This might also drive designs toward self-repair mechanisms. The requirement for redox leveling to prevent the need for large overpotentials highlights the necessity of proton management in any artificial catalyst.

Photoprotection

The antenna–based photoprotection mechanisms, such as those found in natural systems that minimize photodamage by regulating the size of the antenna, dissipating excess light excitation energy and mediating repair, help to avoid and compensate for the oxidative damage inherent in photodriven catalysis in oxygenic photosynthesis. However, it may be that such mechanisms would not be required in DSSCs, with appropriate design maximizing light absorption and structural characteristics that produce robust devices. DSSCs might be inspired by natural photosynthesis, but they are not restrained by the same limits that constrain the natural system.

Concluding Remarks

Energy is the most important issue facing the world in the twenty-first century. Currently, the world still relies heavily on nonrenewable fossil fuels. Solar energy has attracted increasing interest, yet we still lack practical robust working devices for harvesting natural sunlight. Solid–state solar cells are among the very few devices that are commercially available for converting solar energy to electricity. Dye–sensitized solar cells have emerged as promising alternatives to expensive solid–state solar cells.

Another highly desirable use for solar energy is powering fuel generation by water splitting, where chemical fuels (e.g., H_2) can be produced and stored. While some successful examples have been reported in the literature using heterogeneous photocatalysts for visible light-driven water splitting (Maeda et al., 2006; Zou et al., 2001), photoelectrochemical synthesis cells offer advantages such as the effective separation of redox equivalents for solar fuel production. The design of such cells will benefit from a molecular understanding of artificial photosynthetic systems.

There has been rapid progress in mimicking natural photosynthesis, and an exploding body of research in this area holds much promise for improving our understanding of the natural systems and reducing the costs of solar energy conversion. Knowledge gained from research in photosynthesis will greatly facilitate the development of efficient devices leading to the production of affordable and energy-rich fuels from natural sunlight. Grand challenges remain, including the discovery of inexpensive, robust, and efficient water-oxidation catalysts. In addition, limited success has been achieved in coupling single-photon charge separation with well-defined homogenous catalysts.

ACKNOWLEDGMENTS

This work was supported by the National Institutes of Health (GM32715) and the Chemical Sciences, Geosciences, and Biosciences Division, Office of Basic Energy Sciences, Office of Science, U.S. Department of Energy (DE–FG02–07ER15909).

REFERENCES

Abrahamsson, M.L.A., Baudin, H.B., Tran, A., Philouze, C., Berg, K.E., Raymond-Johansson, M.K., Sun, L., Aakermark, B., Styring, S., and Hammarström, L. (2002). Ruthenium-manganese complexes for artificial photosynthesis: Factors controlling intramolecular electron transfer and excited-state quenching reactions. Inorg. Chem. *41*, 1534–1544.

Adir, N. (2005). Elucidation of the molecular structures of components of the phycobilisome: reconstructing a giant. Photosynth. Res. *85*, 15–32.

Ahrens, M.J., Sinks, L.E., Rybtchinski, B., Liu, W., Jones, B.A., Giaimo, J.M., Gusev, A.V., Goshe, A.J., Tiede, D.M., and Wasielewski, M.R. (2004). Self-assembly of supramolecular light-harvesting arrays from covalent multi-chromophore perylene-3,4:9,10-bis(dicarboximide) building blocks. J. Am. Chem. Soc. *126*, 8284–8294.

Alstrum-Acevedo, J.H., Brennaman, M.K., and Meyer, T.J. (2005). Chemical Approaches to Artificial Photosynthesis. 2. Inorg. Chem. *44*, 6802–6827.

Ardo, S., and Meyer, G.J. (2009). Photodriven heterogeneous charge transfer with transition-metal compounds anchored to TiO_2 semiconductor surfaces. Chem. Soc. Rev. *38*, 115–164.

Armstrong, F.A. (2008). Why did Nature choose manganese to make oxygen? Philos. Trans. R. Soc. Lond. B Biol. Sci. *363*, 1263–1270.

Bailey, S., and Grossman, A. (2008). Photoprotection in cyanobacteria: regulation of light harvesting. Photochem. Photobiol. *84*, 1410–1420.

Balzani, V., Bergamini, G., Marchioni, F., and Ceroni, P. (2006). Ru(II)-bipyridine complexes in supramolecular systems, devices and machines. Coord. Chem. Rev. *250*, 1254–1266.

Balzani, V., Credi, A., and Venturi, M. (2008). Photochemical conversion of solar energy. ChemSusChem *1*, 26–58.

Barber, J. (2009). Photosynthetic energy conversion: natural and artificial. Chem. Soc. Rev. *38*, 185–196.

Bekker, A., Holland, H.D., Wang, P.L., Rumble, D., 3rd, Stein, H.J., Hannah, J.L., Coetzee, L.L., and Beukes, N.J. (2004). Dating the rise of atmospheric oxygen. Nature *427*, 117–120.

Berera, R., Herrero, C., van Stokkum, L.H.M., Vengris, M., Kodis, G., Palacios, R.E., van Amerongen, H., van Grondelle, R., Gust, D., Moore, T.A., et al. (2006). A simple artificial light-harvesting dyad as a model for excess energy dissipation in oxygenic photosynthesis. Proc. Natl. Acad. Sci. USA *103*, 5343–5348.

Blankenship, R.E. (2002). Molecular Mechanisms of Photosynthesis (Malden, MA: Blackwell Science Ltd).

Brimblecombe, R., Swiegers, G.F., Dismukes, G.C., and Spiccia, L. (2008). Sustained water oxidation photocatalysis by a bioinspired manganese cluster. Angew. Chem. Int. Ed. Engl. *47*, 7335–7338.

Brudvig, G.W. (2008). Water oxidation chemistry of photosystem II. Philos. Trans. R. Soc. Lond. B Biol. Sci. *363*, 1211–1218.

Cady, C.W., Crabtree, R.H., and Brudvig, G.W. (2008). Functional models for the oxygen-evolving complex of photosystem II. Coord. Chem. Rev. *252*, 444–455.

Cesar, I., Kay, A., Martinez, J.A.G., and Grätzel, M. (2006). Translucent thin film Fe_2O_3 photoanodes for efficient water splitting by sunlight: nanostructure-directing effect of Si-doping. J. Am. Chem. Soc. *128*, 4582–4583.

Chen, H., Faller, J.W., Crabtree, R.H., and Brudvig, G.W. (2004). Dimer-of-dimers model for the oxygen-evolving complex of photosystem II. synthesis and properties of $[Mn^{IV}_4O_5(terpy)_4(H_2O)_2](ClO_4)_6$. J. Am. Chem. Soc. *126*, 7345–7349.

Chen, Z., Concepcion, J.J., Jurss, J.W., and Meyer, T.J. (2009). Single-Site, Catalytic Water Oxidation on Oxide Surfaces. J. Am. Chem. Soc. *131*, 15580–15581.

Chow, W.S., Lee, H.Y., He, J., Hendrickson, L., Hong, Y.N., and Matsubara, S. (2005). Photoinactivation of photosystem II in leaves. Photosynth. Res. *84*, 35–41.

Cogdell, R.J., Gardiner, A.T., Hashimoto, H., and Brotosudarmo, T.H. (2008). A comparative look at the first few milliseconds of the light reactions of photosynthesis. Photochem. Photobiol. Sci. *7*, 1150–1158.

Concepcion, J.J., Jurss, J.W., Templeton, J.L., and Meyer, T.J. (2008). One site is enough. catalytic water oxidation by $[Ru(tpy)(bpm)(OH_2)]^{2+}$ and $[Ru(tpy)(bpz)(OH_2)]^{2+}$. J. Am. Chem. Soc. *130*, 16462–16463.

Deisenhofer, J., and Michel, H. (1989). The photosynthetic reaction center from the purple bacterium *Rhodopseudomonas viridis*. EMBO J. *8*, 2149–2170.

Demmig-Adams, B., Adams, W., and Mattoo, A. (2006). Photoprotection, Photoinhibition, Gene Regulation, and Environment (Dordrecht, The Netherlands: Springer).

Deng, Z., Tseng, H.-W., Zong, R., Wang, D., and Thummel, R. (2008). Preparation and study of a family of dinuclear Ru(II) complexes that catalyze the decomposition of water. Inorg. Chem. *47*, 1835–1848.

Duret, A., and Grätzel, M. (2005). Visible light-induced water oxidation on mesoscopic α-Fe_2O_3 films made by ultrasonic spray pyrolysis. J. Phys. Chem. B *109*, 17184–17191.

Fleming, G.R., and van Grondelle, R. (1997). Femtosecond spectroscopy of photosynthetic light-harvesting systems. Curr. Opin. Struct. Biol. *7*, 738–748.

Frank, H.A., and Brudvig, G.W. (2004). Redox functions of carotenoids in photosynthesis. Biochemistry *43*, 8607–8615.

Fromme, P. (2008). Photosynthetic Protein Complexes A Structural Approach (Weinheim: Wiley-VCH).

Fujishima, A., and Honda, K. (1972). Electrochemical photolysis of water at a semiconductor electrode. Nature *238*, 37–38.

Fujita, E. (1999). Photochemical carbon dioxide reduction with metal complexes. Coord. Chem. Rev. *185-186*, 373–384.

Fujita, E., and Muckerman, J.T. (2008). Catalytic reactions using transition-metal-complexes toward solar fuel production. Bull. Jpn. Soc. Coord. Chem. *51*, 41–54.

Fukuzumi, S., and Kojima, T. (2008). Photofunctional nanomaterials composed of multiporphyrins and carbon-based pi-electron acceptors. J. Mater. Chem. *18*, 1427–1439.

Gall, A., Henry, S., Takaichi, S., Robert, B., and Cogdell, R.J. (2005). Preferential incorporation of coloured-carotenoids occurs in the LH2 complexes from non-sulphur purple bacteria under carotenoid-limiting conditions. Photosynth. Res. *86*, 25–35.

Gao, F., Wang, Y., Shi, D., Zhang, J., Wang, M., Jing, X., Humphry-Baker, R., Wang, P., Zakeeruddin, S.M., and Grätzel, M. (2008). Enhance the optical absorptivity of nanocrystalline TiO_2 film with high molar extinction coefficient ruthenium sensitizers for high performance dye-sensitized solar cells. J. Am. Chem. Soc. *130*, 10720–10728.

Gersten, S.W., Samuels, G.J., and Meyer, T.J. (1982). Catalytic oxidation of water by an oxo-bridged ruthenium dimer. J. Am. Chem. Soc. *104*, 4029–4030.

Golbeck, J.H. (2006). Photosystem I The Light-Driven Plastocyanin: Ferredoxin Oxidoreductase (Dordrecht, The Netherlands: Springer).

Grätzel, M. (2001). Photoelectrochemical cells. Nature *414*, 338–344.

Grätzel, M. (2005). Solar energy conversion by dye-sensitized photovoltaic cells. Inorg. Chem. *44*, 6841–6851.

Gust, D., and Moore, T.A. (1989). Mimicking photosynthesis. Science *244*, 35–41.

Hamann, T.W., Jensen, R.A., Martinson, A.B.F., Van Ryswyk, H., and Hupp, J.T. (2008). Advancing beyond current generation dye-sensitized solar cells. Energy Environ. Sci. *1*, 66–78.

Hambourger, M., Moore, G.F., Kramer, D.M., Gust, D., Moore, A.L., and Moore, T.A. (2009). Biology and technology for photochemical fuel production. Chem. Soc. Rev. *38*, 25–35.

Hammarström, L., and Styring, S. (2008). Coupled electron transfers in artificial photosynthesis. Philos. Trans. R. Soc. Lond. B Biol. Sci. *363*, 1283–1291.

Herrero, C., Lassalle-Kaiser, B., Leibl, W., Rutherford, A.W., and Aukauloo, A. (2008). Artificial systems related to light driven electron transfer processes in PSII. Coord. Chem. Rev. *252*, 456–468.

Herriman, A. (2004). Unusually slow charge recombination in molecular dyads. Angew. Chem. Int. Ed. Engl. *43*, 4985–4987.

Hoff, A.J., and Deisenhofer, J. (1997). Photophysics of photosynthesis. Structure and spectroscopy of reaction centers of purple bacteria. Phys. Rep. *287*, 1–247.

Hu, X., Damjanovic, A., Ritz, T., and Schulten, K. (1998). Architecture and mechanism of the light-harvesting apparatus of purple bacteria. Proc. Natl. Acad. Sci. USA *95*, 5935–5941.

Huang, P., Magnuson, A., Lomoth, R., Abrahamsson, M., Tamm, M., Sun, L., van Rotterdam, B., Park, J., Hammarström, L., Akermark, B., and Styring, S. (2002). Photo-induced oxidation of a dinuclear $Mn_2^{II,II}$ complex to the $Mn_2^{III,IV}$ state by inter- and intramolecular electron transfer to Ru^{III}tris-bipyridine. J. Inorg. Biochem. *91*, 159–172.

Hull, J.F., Balcells, D., Blakemore, J.D., Incarvito, C.D., Eisenstein, O., Brudvig, G.W., and Crabtree, R.H. (2009). Highly active and robust Cp* iridium complexes for catalytic water oxidation. J. Am. Chem. Soc. *131*, 8730–8731.

Hunter, C.N., Daldal, F., Thurnauer, M.C., and Beatty, J.T. (2009). The Purple Phototrophic Bacteria (Dordrecht, The Netherlands: Springer).

Huynh, M.H.V., Dattelbaum, D.M., and Meyer, T.J. (2005). Exited state electron and energy transfer in molecular assemblies. Coord. Chem. Rev. *249*, 457–483.

Imahori, H. (2004). Giant multiporphyrin arrays as artificial light-harvesting antennas. J. Phys. Chem. B *108*, 6130–6143.

Imahori, H., and Fukuzumi, S. (2004). Porphyrin- and fullerene-based molecular photovoltaic devices. Adv. Funct. Mater. *14*, 525–536.

Imahori, H., Mori, Y., and Matano, Y. (2003). Nanostructured artificial photosynthesis. Journal of Photochemistry and Photobiology C: Photochemistry Reviews *4*, 51–83.

Kay, A., Cesar, I., and Graetzel, M. (2006). New benchmark for water photooxidation by nanostructured α-Fe_2O_3 Films. J. Am. Chem. Soc. *128*, 15714–15721.

Kelley, R.F., Lee, S.J., Wilson, T.M., Nakamura, Y., Tiede, D.M., Osuka, A., Hupp, J.T., and Wasielewski, M.R. (2008). Intramolecular energy transfer within butadiyne-linked chlorophyll and porphyrin dimer-faced, self-assembled prisms. J. Am. Chem. Soc. *130*, 4277–4284.

Kiang, N.Y., Siefert, J., Govindjee, and, and Blankenship, R.E. (2007). Spectral signatures of photosynthesis. I. review of earth organisms. Astrobiology *7*, 222–251.

Kodis, G., Herrero, C., Palacios, R., Marino-Ochoa, E., Gould, S., De la Garza, L., Van Grondelle, R., Gust, D., Moore, T.A., Moore, A.L., and Kennis, J.T.M. (2004). Light harvesting and photoprotective functions of carotenoids in compact artificial photosynthetic antenna designs. J. Phys. Chem. B *108*, 414–425.

Koepke, J., Hu, X.C., Muenke, C., Schulten, K., and Michel, H. (1996). The crystal structure of the light-harvesting complex II (B800-850) from *Rhodospirillum molischianum*. Structure *4*, 581–597.

Kopidakis, N., Neale, N.R., and Frank, A.J. (2006). Effect of an adsorbent on recombination and band-edge movement in dye-sensitized TiO_2 solar cells: evidence for surface passivation. J. Phys. Chem. B *110*, 12485–12489.

Kuang, D., Ito, S., Wenger, B., Klein, C., Moser Jacques, E., Humphry-Baker, R., Zakeeruddin Shaik, M., and Grätzel, M. (2006). High molar extinction coefficient heteroleptic ruthenium complexes for thin film dye-sensitized solar cells. J. Am. Chem. Soc. *128*, 4146–4154.

Larkum, T. (1996). How dinoflagellates make light work with peridinin. Trends Plant Sci. *1*, 247–248.

Lewis, N.S. (2007a). Powering the planet. MRS Bull. *32*, 808–820.

Lewis, N.S. (2007b). Toward cost-effective solar energy use. Science *315*, 798–801.

Lewis, N.S., and Nocera, D.G. (2006). Powering the planet: chemical challenges in solar energy utilization. Proc. Natl. Acad. Sci. USA *103*, 15729–15735.

Limburg, J., Vrettos, J.S., Liable-Sands, L.M., Rheingold, A.L., Crabtree, R.H., and Brudvig, G.W. (1999). A functional model for O-O bond formation by the O_2-evolving complex in photosystem II. Science *283*, 1524–1527.

Limburg, J., Vrettos, J.S., Chen, H.Y., de Paula, J.C., Crabtree, R.H., and Brudvig, G.W. (2001). Characterization of the O_2-evolving reaction catalyzed by (terpy)$(H_2O)Mn^{III}(O)_2Mn^{IV}(OH_2)$(terpy) (NO_3) (terpy=2,2′: 6,2″-terpyridine). J. Am. Chem. Soc. *123*, 423–430.

Linsebigler, A.L., Lu, G.Q., and Yates, J.T. (1995). Photocatalysis on TiO_2 surfaces - principles, mechanisms, and selected results. Chem. Rev. *95*, 735–758.

Liu, Z., Yan, H., Wang, K., Kuang, T., Zhang, J., Gui, L., An, X., and Chang, W. (2004). Crystal structure of spinach major light-harvesting complex at 2.72 Å resolution. Nature *428*, 287–292.

Liu, F., Concepcion, J.J., Jurss, J.W., Cardolaccia, T., Templeton, J.L., and Meyer, T.J. (2008). Mechanisms of water oxidation from the blue dimer to photosystem II. Inorg. Chem. *47*, 1727–1752.

Lomoth, R., Magnuson, A., Sjoedin, M., Huang, P., Styring, S., and Hammarström, L. (2006). Mimicking the electron donor side of photosystem II in artificial photosynthesis. Photosynth. Res. *87*, 25–40.

Lubitz, W., Reijerse, E.J., and Messinger, J. (2008). Solar water-splitting into H_2 and O_2: design principles of photosystem II and hydrogenases. Energy Environ. Sci. *1*, 15–31.

Lukas, A.S., Zhao, Y., Miller, S.E., and Wasielewski, M.R. (2002). Biomimetic electron transfer using low energy excited states: A green perylene-based analogue of chlorophyll a. J. Phys. Chem. B *106*, 1299–1306.

Maeda, K., Higashi, M., Lu, D., Abe, R., and Domen, K. (2010). Efficient nonsacrificial water splitting through two-step photoexcitation by visible light using a modified oxynitride as a hydrogen evolution photocatalyst. J. Am. Chem. Soc. *132*, 5858–5868.

Maeda, K., Teramura, K., Lu, D.L., Takata, T., Saito, N., Inoue, Y., and Domen, K. (2006). Photocatalyst releasing hydrogen from water - Enhancing catalytic performance holds promise for hydrogen production by water splitting in sunlight. Nature *440*, 295.

Markvart, T. (2000). Light harvesting for quantum solar energy conversion. Progress in Quantum Electronics *24*, 107–186.

McDaniel, N.D., Coughlin, F.J., Tinker, L.L., and Bernhard, S. (2008). Cyclometalated iridium(III) aquo complexes: efficient and tunable catalysts for the homogeneous oxidation of water. J. Am. Chem. Soc. *130*, 210–217.

McDermott, G., Prince, S.M., Freer, A.A., Hawthornthwaite-Lawless, A.M., Papiz, M.Z., Cogdell, R.J., and Isaacs, N.W. (1995). Crystal-structure of an integral membrane light-harvesting complex from photosynthetic bacteria. Nature *374*, 517–521.

McEvoy, J.P., and Brudvig, G.W. (2006). Water-splitting chemistry of photosystem II. Chem. Rev. *106*, 4455–4483.

Melis, A. (2009). Solar energy conversion efficiencies in photosynthesis: Minimizing the chlorophyll antennae to maximize efficiency. Plant Sci. *177*, 272–280.

Meyer, T.J. (1989). Chemical approaches to artificial photosynthesis. Acc. Chem. Res. *22*, 163–170.

Meyer, G.J. (2005). Molecular approaches to solar energy conversion with coordination compounds anchored to semiconductor surfaces. Inorg. Chem. *44*, 6852–6864.

Michel, H., and Deisenhofer, J. (1987). The photosynthetic reaction center from the purple bacterium *Rhodopseudomonas viridis*. Science *245*, 1463–1473.

Moore, T.A., Gust, D., Mathis, P., Mialocq, J.C., Chachaty, C., Bensasson, R.V., Land, E.J., Doizi, D., Liddell, P.A., Lehman, W.R., et al. (1984). Photodriven charge separation in a carotenoporphyrinquinone triad. Nature *307*, 630–632.

Moore, G.F., Hambourger, M., Gervaldo, M., Poluektov, O.G., Rajh, T., Gust, D., Moore, T.A., and Moore, A.L. (2008). A bioinspired construct that mimics the proton coupled electron transfer between $P680^{\cdot+}$ and the Tyr_Z-His190 pair of photosystem II. J. Am. Chem. Soc. *130*, 10466–10467.

Müller, P., Li, X.-P., and Niyogi, K.K. (2001). Non-photochemical quenching. A response to excess light energy. Plant Physiol. *125*, 1558–1566.

Mullins, C.S., and Pecoraro, V.L. (2008). Reflections on small molecule manganese models that seek to mimic photosynthetic water oxidation chemistry. Coord. Chem. Rev. *252*, 416–443.

Nakamura, Y., Aratani, N., and Osuka, A. (2007). Cyclic porphyrin arrays as artificial photosynthetic antenna: synthesis and excitation energy transfer. Chem. Soc. Rev. *36*, 831–845.

Nantalaksakul, A., Reddy, D.R., Bardeen, C.J., and Thayumanavan, S. (2006). Light harvesting dendrimers. Photosynth. Res. *87*, 133–150.

Nazeeruddin, M.K., De Angelis, F., Fantacci, S., Selloni, A., Viscardi, G., Liska, P., Ito, S., Takeru, B., and Grätzel, M. (2005). Combined experimental and DFT-TDDFT computational study of photoelectrochemical cell ruthenium sensitizers. J. Am. Chem. Soc. *127*, 16835–16847.

O'Regan, B., and Grätzel, M. (1991). A low-cost, high-efficiency solar cell based on dye-sensitized colloidal TiO_2 films. Nature *353*, 737–740.

O'Regan, B.C., Walley, K., Juozapavicius, M., Anderson, A., Matar, F., Ghaddar, T., Zakeeruddin, S.M., Klein, C., and Durrant, J.R. (2009). Structure/function relationships in dyes for solar energy conversion: a two-atom change in dye structure and the mechanism for its effect on cell voltage. J. Am. Chem. Soc. *131*, 3541–3548.

Popovic, Z.D., Kovacs, G.J., Vincett, P.S., Alegria, G., and Dutton, P.L. (1986). Electric-field dependence of the quantum yield in reaction centers of photosynthetic bacteria. Biochim. Biophys. Acta *851*, 38–48.

Poulsen, A.K., Rompel, A., and McKenzie, C.J. (2005). Water oxidation catalyzed by a dinuclear Mn complex: a functional model for the oxygen-evolving center of photosystem II. Angew. Chem. Int. Ed. Engl. *44*, 6916–6920.

Pšenčík, J., Ikonen, T.P., Laurinmaki, P., Merckel, M.C., Butcher, S.J., Serimaa, R.E., and Tuma, R. (2004). Lamellar organization of pigments in chlorosomes, the light harvesting complexes of green photosynthetic bacteria. Biophys. J. *87*, 1165–1172.

Pushkar, Y., Yano, J., Glatzel, P., Messinger, J., Lewis, A., Sauer, K., Bergmann, U., and Yachandra, V. (2007). Structure and orientation of the Mn_4Ca cluster in plant photosystem II membranes studied by polarized range-extended X-ray absorption spectroscopy. J. Biol. Chem. *282*, 7198–7208.

Rappaport, F., and Diner, B.A. (2008). Primary photochemistry and energetics leading to the oxidation of the $(Mn)_4Ca$ cluster and to the evolution of molecular oxygen in Photosystem II. Coord. Chem. Rev. *252*, 259–272.

Rappaport, F., and Lavergne, J. (2001). Coupling of electron and proton transfer in the photosynthetic water oxidase. Biochim. Biophys. Acta *1503*, 246–259.

Reisner, E., Powell, D.J., Cavazza, C., Fontecilla-Camps, J.C., and Armstrong, F.A. (2009). Visible light-driven H_2 production by hydrogenases attached to dye-sensitized TiO_2 nanoparticles. J. Am. Chem. Soc. *131*, 18457–18466.

Ritz, T., Damjanović, A., and Schulten, K. (2002). The quantum physics of photosynthesis. ChemPhysChem *3*, 243–248.

Röger, C., Müller, M.G., Lysetska, M., Miloslavina, Y., Holzwarth, A.R., and Würthner, F. (2006). Efficient energy transfer from peripheral chromophores to the self-assembled zinc chlorin rod antenna: a bioinspired light-harvesting system to bridge the "green gap". J. Am. Chem. Soc. *128*, 6542–6543.

Roszak, A.W., Howard, T.D., Southall, J., Gardiner, A.T., Law, C.J., Isaacs, N.W., and Cogdell, R.J. (2003). Crystal structure of the RC-LH1 core complex from *Rhodopseudomonas palustris*. Science *302*, 1969–1972.

Schuster, D.I., Cheng, P., Jarowski, P.D., Guldi, D.M., Luo, C., Echegoyen, L., Pyo, S., Holzwarth, A.R., Braslavsky, S.E., Williams, R.M., and Klihm, G. (2004). Design, synthesis, and photophysical studies of a porphyrin-fullerene dyad with parachute topology; charge recombination in the Marcus inverted region. J. Am. Chem. Soc. *126*, 7257–7270.

Sens, C., Romero, I., Rodriguez, M., Llobet, A., Parella, T., and Benet-Buchholz, J. (2004). A new Ru complex capable of catalytically oxidizing water to molecular dioxygen. J. Am. Chem. Soc. *126*, 7798–7799.

Serroni, S., Campagna, S., Puntoriero, F., Loiseau, F., Ricevuto, V., Passalacqua, R., and Galletta, M. (2003). Dendrimers made of Ru(II) and Os(II) polypyridine subunits as artificial light-harvesting antennae. C. R. Chimie *6*, 883–893.

Song, H.E., Taniguchi, M., Diers, J.R., Kirmaier, C., Bocian, D.F., Lindsey, J.S., and Holten, D. (2009). Linker dependence of energy and hole transfer in neutral and oxidized multiporphyrin arrays. J. Phys. Chem. B *113*, 16483–16493.

Sproviero, E.M., Gascon, J.A., McEvoy, J.P., Brudvig, G.W., and Batista, V.S. (2008a). A model of the oxygen-evolving center of photosystem II predicted by structural refinement based on EXAFS simulations. J. Am. Chem. Soc. *130*, 6728–6730.

Sproviero, E.M., Gascon, J.A., McEvoy, J.P., Brudvig, G.W., and Batista, V.S. (2008b). Quantum mechanics/molecular mechanics study of the catalytic cycle of water splitting in photosystem II. J. Am. Chem. Soc. *130*, 3428–3442.

Steffen, M.A., Lao, K., and Boxer, S.G. (1994). Dielectric asymmetry in the photosynthetic reaction center. Science *264*, 810–816.

Straight, S.D., Kodis, G., Terazono, Y., Hambourger, M., Moore, T.A., Moore, A.L., and Gust, D. (2008). Self-regulation of photoinduced electron transfer by a molecular nonlinear transducer. Nat. Nanotechnol. *3*, 280–283.

Sturgis, J.N., Tucker, J.D., Olsen, J.D., Hunter, C.N., and Niederman, R.A. (2009). Atomic force microscopy studies of native photosynthetic membranes. Biochemistry *48*, 3679–3698.

Sun, L., Hammarström, L., Åkermark, B., and Styring, S. (2001). Towards artificial photosynthesis: ruthenium-manganese chemistry for energy production. Chem. Soc. Rev. *30*, 36–49.

Tagore, R., Crabtree, R.H., and Brudvig, G.W. (2008). Oxygen evolution catalysis by a dimanganese complex and its relation to photosynthetic water oxidation. Inorg. Chem. *47*, 1815–1823.

Ting, C.S., Rocap, G., King, J., and Chisholm, S.W. (2002). Cyanobacterial photosynthesis in the oceans: the origins and significance of divergent light-harvesting strategies. Trends Microbiol. *10*, 134–142.

Trissl, H.W. (1993). Long-wavelength absorbing antenna pigments and heterogeneous absorption-bands concentrate excitons and increase absorption cross-section. Photosynth. Res. *35*, 247–263.

van Amerongen, H. (2000). Photosynthetic Excitons (Singapore: World Scientific Publishing Co. Pte. Ltd.).

van Brederode, M.E., Jones, M.R., Van Mourik, F., Van Stokkum, I.H.M., and Van Grondelle, R. (1997). A new pathway for transmembrane electron transfer in photosynthetic reaction centers of *Rhodobacter sphaeroides* not involving the excited special pair. Biochemistry *36*, 6855–6861.

van Grondelle, R. (1985). Excitation energy transfer, trapping and annihilation in photosynthetic systems. Biochim. Biophys. Acta *811*, 147–195.

van Grondelle, R., and Novoderezhkin, V. (2001). Dynamics of excitation energy transfer in the LH1 and LH2 light-harvesting complexes of photosynthetic bacteria. Biochemistry *40*, 15057–15068.

van Grondelle, R., Dekker, J.P., Gillbro, T., and Sundstrom, V. (1994). Energy transfer and trapping in photosynthesis. Biochim. Biophys. Acta *1187*, 1–65.

Vasilikiotis, C., and Melis, A. (1994). Photosystem II reaction center damage and repair cycle: chloroplast acclimation strategy to irradiance stress. Proc. Natl. Acad. Sci. USA *91*, 7222–7226.

Wasielewski, M.R. (1992). Photoinduced electron transfer in supramolecular systems for artificial photosynthesis. Chem. Rev. *92*, 435–461.

Wasielewski, M.R. (2006). Energy, charge, and spin transport in molecules and self-assembled nanostructures inspired by photosynthesis. J. Org. Chem. *71*, 5051–5066.

Wiberg, J., Guo, L., Pettersson, K., Nilsson, D., Ljungdahl, T., Mårtensson, J., and Albinsson, B. (2007). Charge recombination versus charge separation in donor-bridge-acceptor systems. J. Am. Chem. Soc. *129*, 155–163.

Wydrzynski, T.J., and Satoh, K. (2005). Introduction. In The Light-Driven Water: Plastoquinone Oxidoreductase, T.J. Wydrzynski, K. Satoh, and J.A. Freeman, eds. (Dordrecht, The Netherlands: Springer).

Yachandra, V.K., Sauer, K., and Klein, M.P. (1996). Manganese cluster in photosynthesis: Where plants oxidize water to dioxygen. Chem. Rev. *96*, 2927–2950.

Yagi, M., Nagoshi, K., and Kaneko, M. (1997). Cooperative catalysis and critical decomposition distances between molecular water oxidation catalysts incorporated in a polymer membrane. J. Phys. Chem. B *101*, 5143–5146.

Yagi, M., Syouji, A., Yamada, S., Komi, M., Yamazaki, H., and Tajima, S. (2009). Molecular catalysts for water oxidation toward artificial photosynthesis. Photochem. Photobiol. Sci. *8*, 139–147.

Yano, J., Kern, J., Sauer, K., Latimer, M.J., Pushkar, Y., Biesiadka, J., Loll, B., Saenger, W., Messinger, J., Zouni, A., and Yachandra, V.K. (2006). Where water is oxidized to dioxygen: structure of the photosynthetic Mn_4Ca cluster. Science *314*, 821–825.

Youngblood, W.J., Lee, S.-H.A., Kobayashi, Y., Hernandez-Pagan, E.A., Hoertz, P.G., Moore, T.A., Moore, A.L., Gust, D., and Mallouk, T.E. (2009). Photoassisted overall water splitting in a visible light-absorbing dye-sensitized photoelectrochemical cell. J. Am. Chem. Soc. *131*, 926–927.

Zinth, W., and Wachtveitl, J. (2005). The first picoseconds in bacterial photosynthesis–ultrafast electron transfer for the efficient conversion of light energy. ChemPhysChem *6*, 871–880.

Zou, Z., Ye, J.H., Sayama, K., and Arakawa, H. (2001). Direct splitting of water under visible light irradiation with an oxide semiconductor photocatalyst. Nature *414*, 625–627.